Vascular Pharmacology 122–123 (2019) 106598

Contents lists available at ScienceDirect

Vascular Pharmacology

journal homepage: www.elsevier.com/locate/vph

Rapid effects of aldosterone on platelets, coagulation, and fibrinolysis lead to experimental thrombosis augmentation

Anna Gromotowicz-Poplawska[a,*], Natalia Marcinczyk[a], Tomasz Misztal[b], Agata Golaszewska[b], Michal Aleksiejczuk[a], Tomasz Rusak[b], Ewa Chabielska[a]

[a] Department of Biopharmacy, Medical University of Bialystok, Poland
[b] Department of Physical Chemistry, Medical University of Bialystok, Poland

ARTICLE INFO

Keywords:
Aldosterone
Thrombosis
Coagulation
Fibrinolysis
Platelet

ABSTRACT

An increase in aldosterone levels positively correlates with an increased risk of acute cardiovascular thrombotic events. The aim of the study was to determine the mechanism of action of prothrombotic aldosterone focusing on the rapid effects of the hormone on platelets, coagulation, and fibrinolysis. A wide panel of advanced *ex vivo* and *in vitro* techniques was used for the evaluation of coagulation and fibrinolysis in aldosterone-treated rats. Additionally, two experimental mice models of thrombosis, which allowed for the intravital observation of the first stage of thrombus formation in real time, were used. Acute administration of aldosterone in rats increased the density of fibrin net and platelet aggregates in clots as well as reduced fibrinolysis. These effects were observed within 10 min and were partially suppressed by eplerenone. Moreover, acute administration of aldosterone in mice enhanced platelet accumulation at the site of endothelial injury induced by laser and increased the area of irreversibly activated platelets in $FeCl_3$-induced thrombus. These results demonstrate that aldosterone acutely affects platelets, coagulation, and fibrinolysis, leading to an enhanced thrombosis. The aldosterone effects were mediated partially *via* a mineralocorticoid receptor. The mechanism seems to involve non-genomic signaling since the effects were observed within a few minutes of aldosterone administration.

1. Introduction

Aldosterone activates both genomic and non-genomic pathways in the cardiovascular system, leading to adverse and harmful effects. Moreover, the classical mineralocorticoid receptor (MR) is believed to be involved in both genomic and rapid, non-genomic signaling. There is a close interaction between the genomic and the non-genomic mechanisms of aldosterone and the non-genomic signaling leads to long-term effects and even supports the genomic action [1–3]. Although the genomic signaling pathway involved in the mechanism of aldosterone action in the cardiovascular system is well described, the non-genomic pathways are still difficult to precisely identify due to the lack of a specific ligand that activates only the non-genomic signaling pathways or an antagonist that selectively blocks only the non-genomic signaling-related receptors [4]. Nevertheless, the rapid effects of aldosterone have been described in cardiovascular tissues. These are involved in ion transport but also in fibrosis, oxidative stress, and inflammation, as well as in the impaired functions of the cardiac system and blood vessels [5–7]. One of the determinants that allow distinguishing the genomic and non-genomic effects of aldosterone is the time of their appearance. Aldosterone has been shown to augment the duration of the monophasic action potential, increase in vascular resistance, and decrease in forearm blood flow within the first 10 min after infusion [8]. Most of these rapid effects of aldosterone were observed in experimental studies with the use of supraphysiological doses of aldosterone that increase the concentration of the hormone as seen in patients with chronic cardiovascular diseases. However, there are some states with acute and highly raised concentrations of aldosterone, for example, during surgery and postoperative period, as seen in patients with coronary artery disease or acute myocardial infarction [9–11]. In addition, the local levels of aldosterone in pathological tissue could be extremely higher than that measured in blood, and thus, the role of the hormone could be

Abbreviations: AUC, area under the curve; CFT, clot formation time; CLT, total time of clot lysis; CT, clotting time; GFP, green fluorescent protein; HUVECs, human umbilical vein endothelial cells; LI, lysis index; MCF, maximum clot firmness; MR, mineralocorticoid receptor; PAI-1, plasminogen activator inhibitor type 1; PPP, platelet-poor plasma; PRP, platelet-rich plasma; PS, phosphatidylserine; TF, tissue factor; t-PA, tissue plasminogen activator; TXB_2, thromboxane B_2; vWF, von Willebrand factor

* Corresponding author at: Department of Biopharmacy, Medical University of Bialystok, Mickiewicza 2c Str., 15-222 Bialystok, Poland.
E-mail address: anna.gromotowicz@umb.edu.pl (A. Gromotowicz-Poplawska).

https://doi.org/10.1016/j.vph.2019.106598
Received 20 May 2019; Received in revised form 9 August 2019; Accepted 19 September 2019
Available online 23 October 2019

difficult to predict. It has been observed that an increase in aldosterone levels positively correlates with an increased risk of acute cardiovascular thrombotic events [12]. This suggests that the acute increase in the level of this hormone is responsible for its rapid non-genomic effect in the hemostatic system, leading to an increased susceptibility to the thrombotic process. In fact, our previous study showed that a 1-h infusion of aldosterone enhanced thrombosis in rats [13]. The aldosterone effect was related to enhanced coagulation, reduced fibrinolysis, increased oxidative stress, and reduced bioavailability of nitric oxide [14]. Furthermore, the prothrombotic action of aldosterone was not completely suppressed by eplerenone, a selective MR antagonist, as well as by valsartan, a selective angiotensin II receptor (AT_1) antagonist [14,15]. These rapid effects of aldosterone, which has only partial sensitivity to the MR and AT_1 antagonists, suggest the involvement of a non-genomic pathway in the mechanism of the prothrombotic action of the hormone. Therefore, the aim of the present study was to extend our previous research and determine the mechanism of aldosterone action in the hemostatic system, focusing on the rapid effects of the hormone that may enhance the thrombotic process. Taking into account that the interaction of platelets and the vascular wall is a key step that promotes thrombus formation, this study investigated the early effects of aldosterone on the above components of the hemostatic system. Moreover, we evaluated the role of MR, since the direct effects of aldosterone on hemostasis involve the presence of its specific receptor in the target cells. The expression of MR is not just limited to the kidneys. At both mRNA and protein level, MR expression has been demonstrated in the heart [16,17], but also in the blood vessels—vascular smooth muscle cells, fibroblasts, and endothelial cells—as well as in human platelets [18–20]. It was also shown that the tissue-specific 11β-hydroxysteroid dehydrogenase of type 2 (11β-HSD2), which transforms glucocorticoids into inactive metabolites allowing for the selective stimulation of MRs by aldosterone, is expressed the sites of cardiovascular MR expression (*e.g.* vascular smooth muscle cells, endothelial cells) [21,22]. Thus, we assumed that the hemostatic system, which involves vascular wall, endothelium and platelet interactions, could be a target for direct MR-dependent aldosterone actions.

We used a wide panel of advanced techniques, which allowed for a more comprehensive evaluation of aldosterone effects on hemostatic system. The results of this study extend our previous findings regarding the acute effects of aldosterone on thrombotic process in rats. Here, we used the blood and plasma, as well as the human umbilical vein endothelial cells (HUVECs), for a wide evaluation of the *ex vivo* and *in vitro* function of platelets, and the processes of coagulation and fibrinolysis. In the experiments with rats, we used aldosterone at a dose of 30 μg/kg, which was found to be the strongest prothrombotic dose in our previous *in vivo* study [14,15]. Additionally, we used two experimental mice models of thrombosis, which allowed for the intravital observation of the first stage of thrombus formation in real time with confocal microscopy. We assume that these models are the most appropriate for the confirmation and evaluation of the rapid effects of aldosterone, since the hormone effects could be visualized only in the very first minutes.

2. Materials and methods

2.1. Animals

Wistar rats (250–300 g, 98 male), wild-type C57BL/6 J/cmbd mice (20–23 g, 48 male), and transgenic C57BL/6-Tg(CAG-EGFP)1Osb/J/cmbd mice (20–23 g, 60 male) expressing green fluorescent protein (GFP) were used. The transgenic mouse line, with an “enhanced” GFP (EGFP) cDNA under the control of a chicken beta-actin promoter and a cytomegalovirus enhancer, exhibits widespread EGFP fluorescence in all cells and tissues, with the exception of erythrocytes and hair. The mice were purchased from Jackson Laboratory and maintained at the Center of Experimental Medicine of Medical University of Bialystok (Poland). All the animals were housed in group cages as appropriate, in a room with a 12-h light/dark cycle, and allowed access to tap water and standard rat/mouse food. Procedures involving the animals and their care were conducted according to the institutional guidelines that are in compliance with the national and international laws, including EU Directive 2010/63/EU for animal experiments and the guidelines for the care and use of laboratory animals in biomedical research. Before starting the experimental procedures, the rats were anesthetized with pentobarbital (Morbital; Biovet, Poland, 50 mg/kg, *i.p.*) and mice with the mixture of ketamine (Ketamina 10%; Biowet, Poland, 120 mg/kg, *i.p.*) and xylazine (Xylapan; Biowet, Poland, 12.5 mg/kg, *i.p.*). All the procedures were approved by the Local Ethical Committee of Animal Testing at the Medical University of Bialystok (permit numbers: 9/2015, 93/2018, 94/2018).

2.2. Antibodies and chemicals

Alexa Fluor™ 647 Annexin V conjugate (Thermo Fisher Scientific, USA), human recombinant tissue factor (Innovin, Dade Behring, Germany), native human Glu-plasminogen (Enzyme Research Laboratories, USA), Alexa Fluor 488 human fibrinogen conjugate (Thermo Fisher Scientific, USA), eplerenone (Inspra; Pfizer, UK), collagen (Chronolog, USA), low-serum growth supplement (LSGS; Cascade Biologics Inc., UK), and Medium 200 (M200; Cascade Biologics Inc., UK) were used. Acetylsalicylic acid (ASA), aldosterone, apyrase, bovine albumin, calcium chloride, DiOC6(3) (3′,3′-dihexyloacarbocyanidine iodide), ferric chloride ($FeCl_3$), HEPES (N-(2-hydroxyethyl)piperazine-N′-(2-ethanosulfonic acid)), penicillin, streptokinase, streptomycin, trypsin, and trypan blue were purchased from Sigma-Aldrich (Poland). Citric acid, dimethyl sulfoxide (DMSO), ethylenediaminetetraacetic acid (EDTA), ethanol, glucose, magnesium chloride, natrium chloride, phosphate-buffered saline (PBS), potassium chloride, sodium bicarbonate, sodium phosphate, and trisodium citrate were purchased from Polish Chemicals Reagents (Poland). Glu-plasminogen was labeled using Alexa Fluor 647 Protein Labeling Kit (Thermo Fisher Scientific, USA).

2.3. Ex vivo evaluation of clot structure with confocal microscopy

Rats were anesthetized, and aldosterone or its vehicle (0.04% ethanol) was administered in a single bolus into the left femoral vein. Aldosterone was used at a dose of 30 μg/kg, which was found to induce the strongest prothrombotic effect in rats in our previous study [14]. Eplerenone, a selective MR antagonist, was administered *per os* using an oral-gastric feeding tube, at a single dose of 100 mg/kg (in 5% aqueous gum arabic solution) 30 min prior to aldosterone administration. After 10 min of aldosterone injection, blood samples were drawn from the right ventricle of the heart and mixed with 3.13% sodium citrate in a volume ratio of 9:1. Platelet-rich plasma (PRP) was obtained by centrifugation of the whole blood at 200 × *g* for 20 min. To prepare platelet-poor plasma (PPP), PRP was centrifuged at 14,000 × *g* for 5 min. Fibrin and platelet–fibrin clots were prepared and visualized using a confocal microscope as previously described [23]. One PRP clot and one PPP clot were prepared from the blood sample of each animal. In brief, samples of PPP or PRP were preincubated with Alexa Fluor 488-labeled human fibrinogen (added to a final concentration of 16 μg/mL) and clotting was triggered by recalcification. Samples were examined after 2 h of incubation (time taken to complete the gelation process) at 37 °C on microchamber slides (Ibidi μ-slide VI; Thistle Scientific). Alexa Fluor 488-labeled human fibrinogen was excited by a 488-nm laser beam (LaserStack 488 nm, 3iL33; Intelligent Imaging Innovations, Inc., USA). Pictures were taken using a fixed-stage Zeiss Axio Examiner Z.1 microscope equipped with a W Plan-Apochromat 20 × /1.0 water immersion objective. At least five pictures of different areas of each clot were taken, and one representative image is presented. Relative clot density was established in each picture as the number of fibers crossing

a single, randomly placed 30-μm-long straight line, and then the average from five measurements was calculated and showed as one dot in the graph. In the case of PRP-derived clots, platelet-rich and platelet-free zones were analyzed separately (an example shown in Suppl. Fig. 1).

2.4. Ex vivo evaluation of coagulation and fibrinolysis with thromboelastometry

Thromboelastometric measurements were performed on the ROTEM® system (Tem International GmbH, Mannheim, Germany) as described previously in our study [23,24]. For the *ex vivo* evaluation of coagulation and fibrinolysis, we used whole blood from the rats administered with single-bolus aldosterone (30 μg/kg) or vehicle; some of the rats received a single eplerenone dose (100 mg/kg) *per os* 30 min before aldosterone administration. After 10 min of aldosterone injection, blood samples were drawn and mixed with 3.13% sodium citrate (9:1). ROTEM analysis was started 30 min after the blood was drawn by adding 320 μL of blood to a cuvette already containing 20 μL of re-calcification reagents. For evaluating the kinetics of coagulation, the samples were recalcified (final $CaCl_2$ concentration of 10 mM), whereas fibrinolytic potential was assessed using an additional 140 ng/mL tissue factor (TF) and 40 IU/mL streptokinase. We measured the following parameters: clotting time (CT)—the time from the start of the measurement to the beginning of the fibrin polymerization process; clot formation time (CFT)—the time from CT until a clot firmness of 20-mm point was reached; alpha angle (α)—the angle showing the dynamics of clot formation; maximum clot firmness (MCF)—a parameter reflecting the strength of the formed clot; percentage reduction of MCF in time (LI_{30}, LI_{45}, LI_{60}—lysis index at 30, 45, and 60 min); and the total time of clot lysis (CLT).

2.5. Platelet adhesion to collagen in vitro

Blood was collected from the anesthetized healthy rats. Then, a washed platelet suspension was prepared as previously described [14]. The final concentration of platelets in the washed platelet samples was found to be 3×10^5 platelets/μL. Platelet adhesion to fibrillar collagen was carried out according to the method of Mant [25]. Briefly, 250 μL of the washed platelet samples was incubated in an Elvi aggregometer at 37 °C and stirred at 900 rpm with EDTA (5 mM) to prevent platelet aggregation. After 5 min of preincubation, aldosterone (10^{-8}–10^{-5} M) or vehicle (ethanol 10^{-5} M) was added and the incubation was continued for another 10 min. Then, collagen (50 μg/mL) was added, and the platelets were incubated for a further 10 min. The platelets were counted optically before and after collagen addition in a Bürker chamber after dilution with the Unpette system. Platelet adhesion index was calculated using the formula: [(platelet count before adding the collagen-platelet count after adding the collagen)/platelet count before adding the collagen] × 100%.

2.6. Platelet aggregation in vitro

Blood was collected from the anesthetized healthy rats. The citrated whole blood (500 μL) was preincubated with aldosterone (10^{-8}–10^{-5} M) or vehicle (ethanol 10^{-5} M) for 10 min, and then collagen (5 μg/mL) was added and the aggregation trace was recorded for 6 min. The collagen-stimulated platelet aggregation was evaluated following the impedance method as previously described using a Whole Blood Lumi-Aggregometer (Chronolog, USA) [26].

2.7. Dynamic generation of thromboxane B_2 (TXB_2)

Dynamic generation of TXB_2 was achieved as previously described [27]. Briefly, TXB_2 was generated in 500 μL of citrated whole-blood samples collected from the healthy rats. Samples were diluted with 0.9% NaCl in a 1:1 (*v*/v) ratio and preincubated with aldosterone (10^{-8}–10^{-5} M) or vehicle (ethanol 10^{-5} M) for 10 min. Then, samples were vigorously stirred with alternating rotating cycles (three rotations to the left and then three rotations to the right) in aggregometer cuvettes at 37 °C and 1000 rpm. As shown previously, these alternating rotating cycles provide enough shear force to evoke TXB_2 generation and platelet aggregation during the time course of the experiments [27,28]. After 10 min of stirring, 200 μL of blood was drawn off and mixed with 200 μL of a cold solution of ASA (500 μL) to stop the further generation of TXB_2. The concentration of TXB_2 in the plasma was analyzed using an ELISA kit (Enzo Life Sciences, UK) and a microplate reader ELx808 (BioTek Instruments, Inc., USA).

2.8. Coagulation and fibrinolysis evaluation in HUVECs

Cryopreserved HUVECs (Cascade Biologics Inc., UK) were used for the evaluation of coagulation and fibrinolysis. Briefly, the cells were grown in M200 supplemented with penicillin (100 U/mL), streptomycin (100 mg/mL), and LSGS at 37 °C in a 95% humidified atmosphere of 5% CO_2. The medium was replaced every 2–3 days. At confluence, the cells were subcultured by trypsinization, after which they were seeded at a split ratio of 1:3. Cellular viability was determined using trypan blue staining method [29]. Cultures at 4–5 passages were used in the experiments. The HUVECs were divided into three experimental groups and cultured at 37 °C in medium: 1) control—cells in a medium without any addition, 2) cells in a medium incubated with vehicle, and 3) cells in a medium incubated with aldosterone (10^{-7} M). After 10 and 120 min, cell supernatants were collected and the antigen levels of TF, von Willebrand factor (vWF), tissue plasminogen activator (t-PA), and plasminogen activator inhibitor type 1 (PAI-I) were measured using commercial ELISA test kits (Innovative Research, USA).

2.9. Intravital imaging

Intravital confocal fluorescence microscopy was performed as described previously [30,31]. For intravital observation of platelet activity within the thrombus forming inside the mesenteric venule of a mouse, a fixed-stage Zeiss Axio Examiner Z.1 microscope (Carl Zeiss Microscopy GmbH, Germany) was used. An objective (W Plan-Apochromat 20×/1.0 water immersion objective; Carl Zeiss Microscopy GmbH, Germany) was applied. In our study, confocal imaging involved the laser excitation of fluorescent agents (LaserStack 488 nm, LaserStack 640 nm, 3iL33; Intelligent Imaging Innovations, Inc., USA), matched to a multiband emission filter (537/694 Dualband Emitter H; AHF Analysentechnik, Germany), with the use of a high-speed confocal scanner (Confocal Scanner Unit CSU-X1; Yokogawa Electric Corporation, Japan), and the intensified images were captured on a high-speed digital CCD camera (C9300-221; Hamamatsu, Japan). The thrombus formation and its progression were imaged in one focal plane (2D imaging) corresponding to the largest area of the thrombus. Collected images (four images per second) were analyzed using SlideBook 6 (Intelligent Imaging Innovations, Inc., USA).

2.10. Intravital thrombosis models

Two different mouse models of thrombosis—laser-induced and $FeCl_3$-induced thrombosis—were used, and intravital observation was carried out in confocal mode [30–32].

2.10.1. Laser-induced thrombosis in mice

GFP mice were anesthetized, and the mesenteric venules were isolated. The mesentery was continuously perfused with warm PBS (37 °C) to prevent the vessels from drying and to ensure immersion. Aldosterone (10, 30, 100, and 200 μg/kg; 50 μL) or its vehicle (0.04% ethanol; 50 μL) was injected in a single bolus into the right femoral vein. Eplerenone was administered *per os* at a dose of 100 mg/kg 30 min

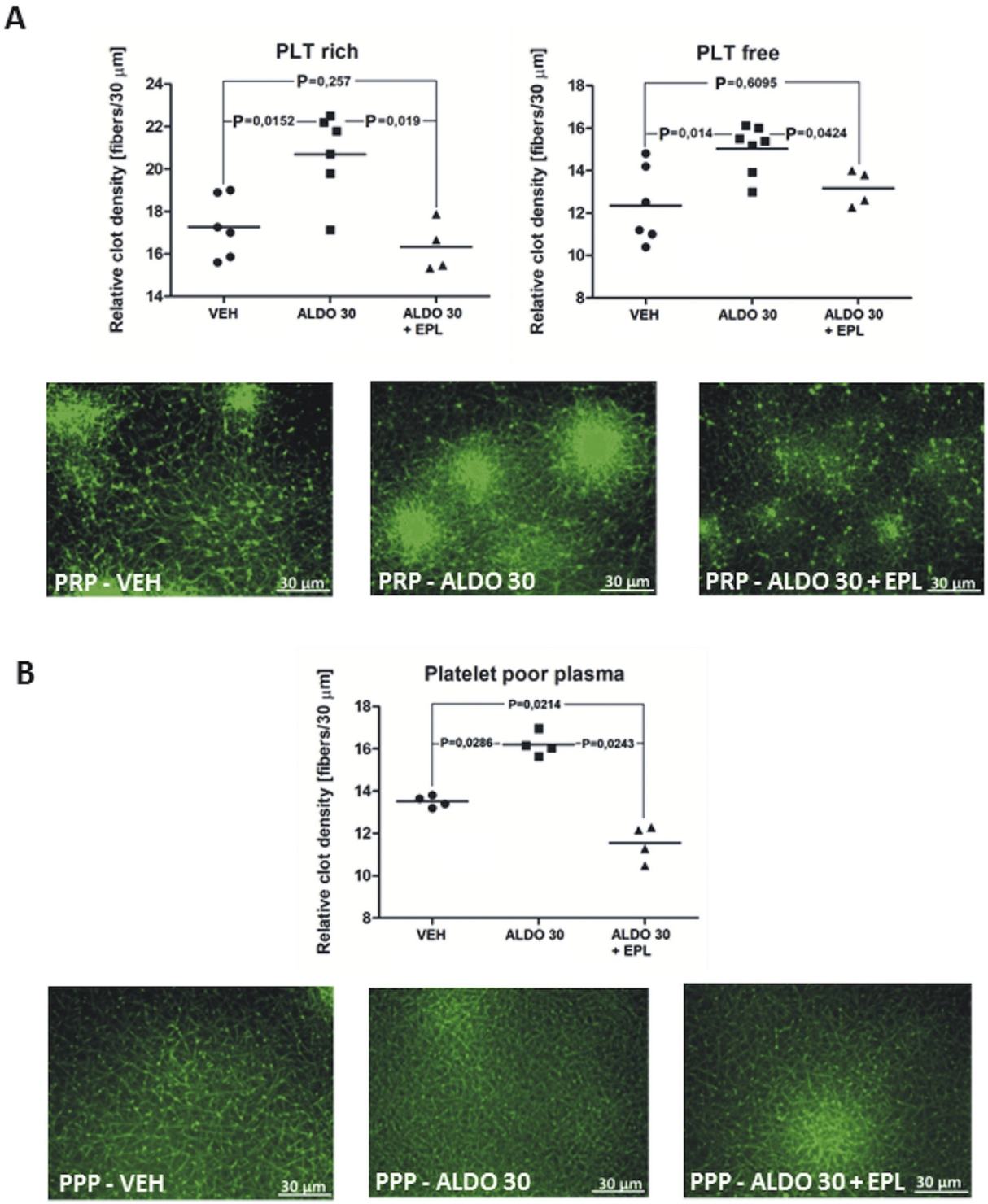

Fig. 1. The effect of aldosterone on the structure of platelet–fibrin clots in the blood plasma obtained from rats treated acutely with vehicle (VEH), aldosterone (ALDO, 30 μg/kg), and eplerenone (EPL, 100 mg/kg): A) the relative clot density in the platelet-rich plasma (PRP) (platelet-rich zones on the left, platelet-free zones on the right), and representative confocal images showing a structure of platelet–fibrin clots; B) the relative clot density in the platelet-poor plasma (PPP), and representative confocal images showing a structure of platelet–fibrin clots. Data are presented as mean ± SEM, magnification 20×; n = 4–6.

before aldosterone administration. After 5 min of aldosterone injection, an endothelial injury was induced using a 512-nm argon-ion laser. The laser beam was focused on the endothelium through the objective lens of the microscope [30,31]. During the experiment, GFP was excited by a 488-nm laser (LaserStack 488 nm, 3iL33; Intelligent Imaging Innovations, Inc., USA). The early stage of thrombus formation, observed as platelet accumulation at the site of endothelial injury, was imaged for 8 min. The rate of thrombus formation was measured as the relative fluorescence intensity of GFP over time, and then calculated as the area under the curve (AUC) using TP4.1 pharmacometric software (ThothPro™, Poland).

2.10.2. *$FeCl_3$-induced thrombosis in mice*

Wild-type mice were anesthetized, and the mesenteric venules were

Table 1
The effect of aldosterone on the kinetics of coagulation and fibrinolysis in the whole blood of rats treated acutely with vehicle (VEH), aldosterone (ALDO, 30 μg/kg), and eplerenone (EPL, 100 mg/kg), measured with thromboelastometry.

	Coagulation				Fibrinolysis			
	CT	CFT	α angle	MCF	LI_{30}	LI_{45}	LI_{60}	CLT
	[s]	[s]	[°]	[mm]	[%]	[%]	[%]	[min]
VEH	334 ± 37	83 ± 4	74 ± 3	72 ± 2	90 ± 5	60 ± 15	35 ± 11	77 ± 7
ALDO 30	293 ± 37	66 ± 9	78 ± 2	74 ± 2	99 ± 1	96 ± 3*	93 ± 4**	165 ± 15**
ALDO 30 + EPL	347 ± 40	87 ± 14	73 ± 3	69 ± 2	96 ± 1	63 ± 16†	36 ± 18††	92 ± 23†

Data are presented as mean ± SEM. $n = 8$. CT—clotting time; CFT—clot formation time; MCF—maximum clot firmness; LI_{30}, LI_{45}, and LI_{60}—lysis index at 30, 45, and 60 min; CLT—total time of clot lysis.
* $p < .05$.
** $p < .01$ *vs* VEH.
† $p < .05$.
†† $p < .01$ *vs* ALDO 30.

isolated. Aldosterone (100 μg/kg) or vehicle was injected in a single bolus into the right femoral vein. Eplerenone (100 mg/kg) was administered *per os* in a single dose 30 min prior to aldosterone administration. To visualize the irreversible platelet activation, Alexa Fluor 647-labeled Annexin V (2 mg/g in 50 μL PBS) was immediately injected into the left femoral vein. To visualize the vessel wall, partially activated platelets, and nonactivated platelets, the DiOC6(3) (0.1 mM in 50 μL of the mixture of DMSO and PBS; volume ratio 1:50) was administered by intramuscular injection. The final concentration of DMSO in the solution of DiOC6(3) that was administered to the mice (all groups) was 0.02% (v/v). According to the *in vivo* and *in vitro* data it is recommended to keep DMSO concentration at 1% or less [32,33]. After 5 min of aldosterone injection, a vessel wall injury was induced with $FeCl_3$ (20% solution, 0.1 μL) that was applied topically on the adventitial surface of a blood vessel [34]. During the experiment, Annexin V was excited by a 640-nm laser and DiOC6(3) was excited by a 488-nm laser (LaserStack 488 nm, LaserStack 640 nm, 3iL33; Intelligent Imaging Innovations, Inc., USA). The regions of fluorescence (corresponding to the labeled thrombi structures) were encircled every 30 s of the recording of a particular image. The areas of regions from one thrombus were calculated with SlideBook 6 and then added up.

2.11. In vivo evaluation of fibrinolysis in mice

Wild-type mice were anesthetized, injected with aldosterone (100 μg/kg) or vehicle, and prepared for $FeCl_3$-induced thrombosis. Immediately after aldosterone administration (5 min before the induction of vessel wall injury with $FeCl_3$), native human plasminogen with glutamic acid at the N-terminus (Glu-plasminogen) was injected into the left femoral vein. Glu-plasminogen was administered at a final concentration of 0.8 μM, which was sufficient to fully visualize the fibrin incorporated into thrombus [35]. The ratio of exogenous to endogenous plasminogen was 1:1. During the experiment, Glu-plasminogen was excited by a 640-nm laser. The fluorescence of Glu-plasminogen within the formed thrombi was observed within 6 min. The drop in the intensity of the red fluorescence corresponding to fibrin dissolution and Glu-plasminogen diffusion was calculated as a percent of the fluorescence decrease within 6 min of observation (0′–6′ min).

2.12. Data analysis

The data are presented as mean ± SEM of the number of determinations (n). Statistical analysis was performed using the Mann–Whitney test. Differences were considered significant at a *p*-value < .05. All analyses were done in GraphPad Prism 5. The relative fluorescence intensity over time was calculated as AUC using TP4.1 pharmacometric software (ThothPro™, Poland).

3. Results

3.1. The effect of aldosterone on the structure of platelet–fibrin clots

In our previous study, we showed that acute infusion of aldosterone at a dose of 30 μg/kg enhanced the thrombus mass in rats *in vivo* [14]. Here, we evaluated the effect of acute injection of aldosterone at a dose of 30 μg/kg on the structure of platelet–fibrin clots formed *ex vivo* in rat plasma (Fig. 1). The relative clot density evaluated using a confocal microscope showed a significant increase in the aldosterone group compared to the vehicle-treated group. Moreover, the aldosterone effect was comparable in both PRP (Fig. A1) and PPP (Fig. B1). Fibrin mesh, which was formed in the presence of both aldosterone and eplerenone, was reduced and showed a similar structure to that of the vehicle-treated rats in both PRP and PPP. Thus, aldosterone acutely affects not only the mass but also the structure of the thrombus *via* an MR-dependent mechanism.

3.2. The effect of aldosterone on the kinetics of clot formation and fibrinolysis ex vivo

In the next set of *ex vivo* experiments, the acute effect of aldosterone at a dose of 30 μg/kg on coagulation and fibrinolysis was determined in rat blood. The results of thromboelastometry showed that aldosterone did not change significantly the coagulability of whole blood from rats (Table 1). However, more significant changes were observed in fibrinolysis. The duration of lysis (LI at 30–60 min) and CLT were also markedly prolonged in the aldosterone group. Pretreatment with eplerenone eliminated the fibrinolysis resistance induced by aldosterone (Table 1). Thus, the observed acute effect of aldosterone on the mass and structure of the thrombus may result from fibrinolysis inhibition.

3.3. The effect of aldosterone on platelet activation in vitro

In our previous study, we showed that aldosterone administered at a dose of 30 μg/kg significantly increased platelet adhesion to collagen *ex vivo* [14]. In the present study, we determined the acute effect of aldosterone on platelet activation *in vitro*. We found that at a range of concentrations of 10^{-8}–10^{-5} M, aldosterone caused no changes in platelet adhesion to collagen, collagen-induced aggregation, or TXB_2 generation (Table 2). This suggests that platelets do not respond to aldosterone action *in vitro*.

3.4. The effect of aldosterone on coagulation- and fibrinolysis-related factors in endothelial cells

Considering that endothelium plays an important role in the

Table 2
The acute effect of aldosterone (ALDO, 10^{-8}–10^{-5} M) on the adhesion of rat platelets to collagen, collagen-induced aggregation, and dynamic thromboxane B_2 (TXB_2) generation in platelets *in vitro*.

	VEH	ALDO	ALDO	ALDO	ALDO
		10^{-8} M	10^{-7} M	10^{-6} M	10^{-5} M
Adhesion [%]	36.2 ± 2.8	36.8 ± 2.1	37.2 ± 1.3	37.5 ± 2.8	36.4 ± 3.0
Aggregation [Ω]	6.2 ± 0.7	5.9 ± 0.3	5.7 ± 0.3	6.1 ± 0.4	5.8 ± 0.2
TBX_2 generation [pg/ml]	0.56 ± 0.13	0.58 ± 0.11	0.62 ± 0.12	0.65 ± 0.14	0.52 ± 0.09

Data are presented as mean ± SEM; $n = 8$.

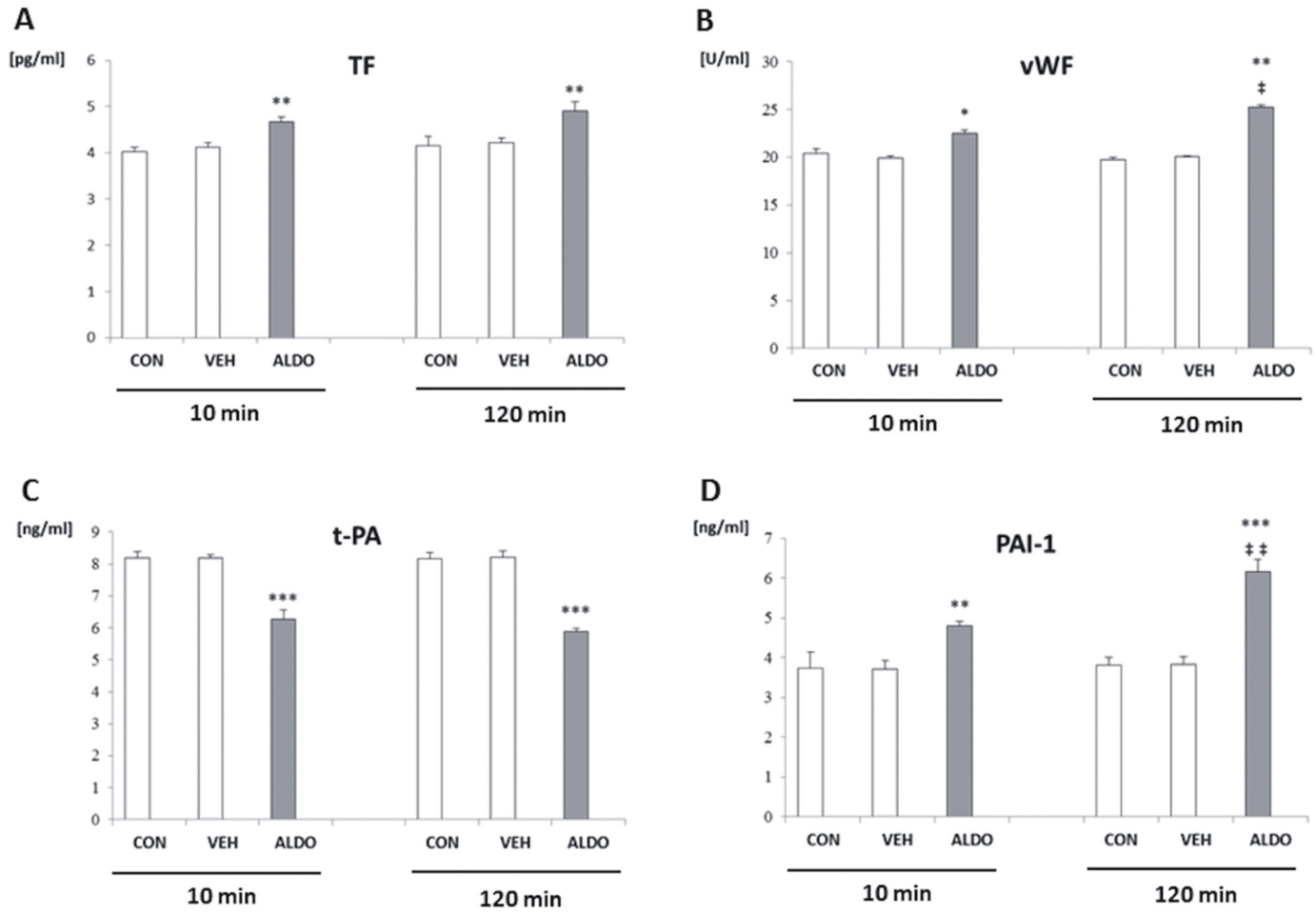

Fig. 2. The effect of aldosterone on coagulation and fibrinolytic factors in the human umbilical vein endothelial cells (HUVECs). Cell supernatants were collected from the unstimulated HUVECs (CON), and the HUVECs stimulated with vehicle (VEH) and aldosterone (ALDO 10^{-7} M) for 10 and 120 min for measuring the antigen levels of A) tissue factor (TF), B) von Willebrand factor (vWF), C) tissue plasminogen activator (t-PA), and D) plasminogen activator inhibitor type 1 (PAI-1). Data are presented as mean ± SEM; *$p < .05$, **$p < .01$, ***$p < .001$ *vs* VEH; ‡$p < .05$, ‡‡$p < .01$ *vs* ALDO 10 min; $n = 8$.

regulation of thrombus formation, in the next set of *in vitro* experiments, the acute effect of aldosterone on endothelium-dependent coagulation and fibrinolysis was determined. The results showed that preincubation of HUVECs with aldosterone (10^{-7} M) for 10 min increased the secretion of TF ($p < .01$), vWF ($p < .05$), and PAI-1 ($p < .01$) and reduced the release of t-PA ($p < .001$). However, preincubation of HUVECs with aldosterone for 120 min did not further affect the secretion of TF and t-PA, although it increased the secretion of vWF ($p < .05$) and PAI-1 ($p < .01$) compared to that observed with 10-min incubation (Fig. 2). These results confirm that within 10 min aldosterone affects the secretion of procoagulants and antifibrinolytic factors from endothelial cells, leading to hemostatic imbalance.

3.5. The effect of aldosterone on laser-induced thrombosis in mice

To confirm and identify the mechanism of the acute effect of aldosterone on the interaction between platelets and endothelium, thrombosis was induced in GFP mice using laser and the early step of thrombus formation was intravitally observed. The results showed that the acute injection of aldosterone at a dose of 10 and 30 μg/kg had no effect on laser-induced thrombosis, whereas aldosterone administered at a dose of 100 μg/kg significantly increased platelet accumulation at the site of endothelial injury compared to that measured in the vehicle-injected mice (Fig. 3, Vid. 1, Vid. 2). The aldosterone effect was observed intravitally within 8 min of laser injury. A significant increase was observed in the fluorescence intensity of accumulated platelets, calculated as AUC, in the aldosterone group compared to vehicle-

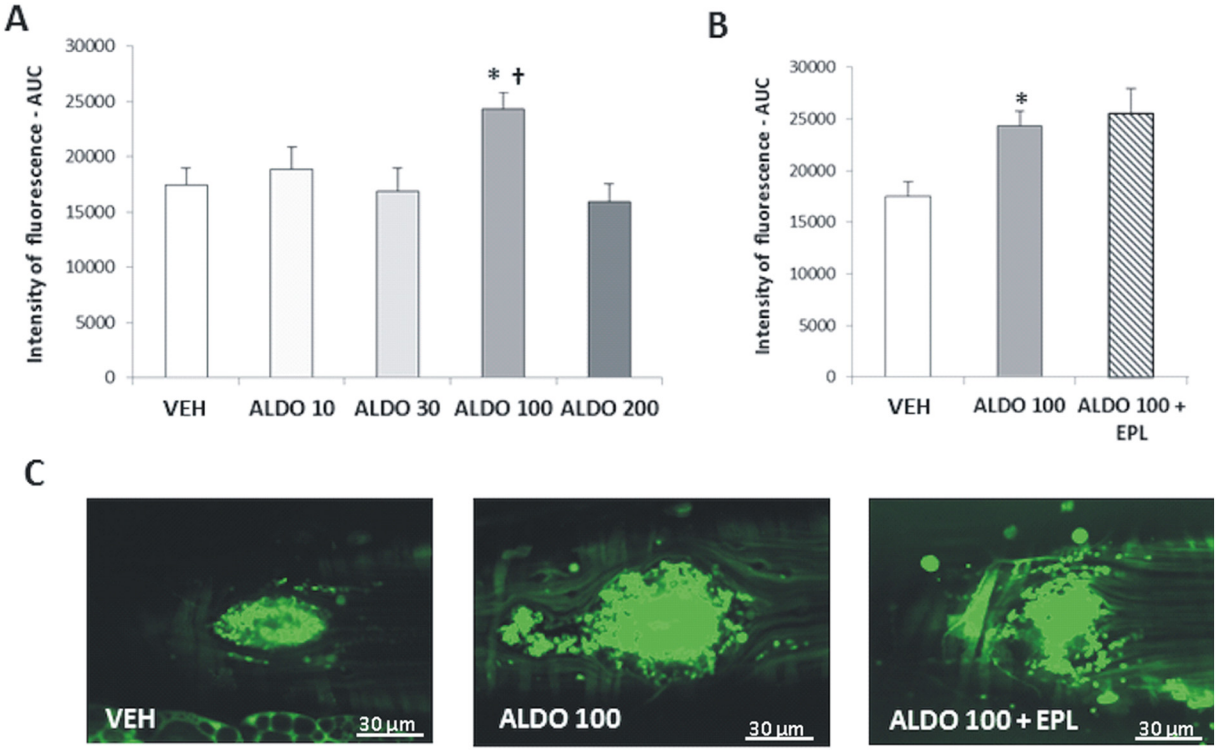

Fig. 3. The effect of aldosterone on platelets accumulation during thrombus formation in the green fluorescent protein (GFP) mice with laser-induced thrombosis: A, B) expressed as relative fluorescence intensity of GFP from platelet thrombus in the mice treated acutely with vehicle (VEH), aldosterone (ALDO 10, 30, 100, and 200 µg/kg), and eplerenone (EPL 100 mg/kg) calculated as an area under the curve (AUC); C) presented as confocal images of the formed platelet thrombus 2 min after laser-induced injury (representative images, blood flow from the right to the left, objective 20×). Data are presented as mean ± SEM; *$p < .05$ *vs* VEH; †$p < .05$ *vs* ALDO 30; $n = 8$. (For interpretation of the references to colour in this figure legend, the reader is referred to the web version of this article.)

treated mice ($p < .05$; Fig. A3). The MR blockade achieved with a single dose of eplerenone did not reduce aldosterone-increased platelet accumulation (Fig. B3). However, the highest dose of aldosterone (200 µg/kg) did not affect platelet accumulation, although a simultaneous increase in blood flow was observed in the mesenteric vessel (Vid. 3). Thus, aldosterone affects platelet accumulation at the site of endothelial injury *in vivo* within 10 min, and the strongest effect on this first stage of thrombus formation is produced by aldosterone at a dose of 100 µg/kg.

3.6. The effect of aldosterone on platelet activation in $FeCl_3$-induced thrombosis in mice

To assess the effect of aldosterone on the irreversible platelet activation, thrombosis was induced in wild-type mice using $FeCl_3$. The results showed that the acute injection of aldosterone at a dose of 100 µg/kg significantly increased the irreversible platelet activation within the $FeCl_3$-induced thrombus in mice (Fig. 4). The area of irreversible activated platelets, expressing phosphatidylserine (PS) on their surface (PS-positive platelets, red fluorescence), was significantly increased in mice injected acutely with aldosterone compared to vehicle-treated mice ($p < .001$; Fig. A4). Pretreatment with a single dose of eplerenone significantly reduced the increase in irreversible platelet activation caused by aldosterone ($p < .001$; Fig. A4, Fig. B4). These results confirm that aldosterone acutely enhances the irreversible platelet activation *via* an MR-dependent mechanism.

3.7. The effect of aldosterone on in vivo fibrinolysis in mice

To verify if fibrinolysis *in vivo* is affected acutely by aldosterone and simultaneously with platelet activation, thrombosis was induced using $FeCl_3$ in wild-type mice injected with labeled Glu-plasminogen. The results showed that the acute injection of aldosterone at a dose of 100 µg/kg did not significantly change the distribution of Glu-plasminogen within the $FeCl_3$-induced thrombus in mice (Fig. 5). The drop in the intensity of red fluorescence exhibited by Glu-plasminogen within 6 min of thrombosis induction was more pronounced in the vehicle-treated mice (over 17%) than in the aldosterone-treated group (10%), suggesting the reduced effectiveness of fibrinolysis in the aldosterone-injected mice.

4. Discussion

In the present study, we have shown for the first time that the prothrombotic action of aldosterone is related to its early and rapid effects in the hemostatic system, which increase the susceptibility to thrombosis. We have also shown that the interaction of platelets and the vascular wall is a key step in the acute aldosterone-enhanced thrombus formation and its progression. Moreover, we confirm that the rapid action of aldosterone also affects the plasma- and endothelium-dependent coagulation and fibrinolysis. We observed that the acute effects of aldosterone were partially mediated *via* MR. Bearing in mind that the aldosterone effects were observed within a few minutes, we suggest that the non-genomic signaling plays a role in the mechanism of action of this hormone.

We found that aldosterone altered the structure of platelet–fibrin clots *via* an MR-dependent mechanism. An altered clot structure may result in the formation of thrombi that are mechanically more stable, and thus more resistant to fibrinolysis. In particular, clots formed in the aldosterone group were much denser and more cross-linked, in both PRP and PPP. This may also have resulted from the faster thrombin formation, since we observed a shortening of CFT by 20% in the aldosterone group. As no exogenous thrombin was used in the experiments, the clot structure observed seemed to be the result of the

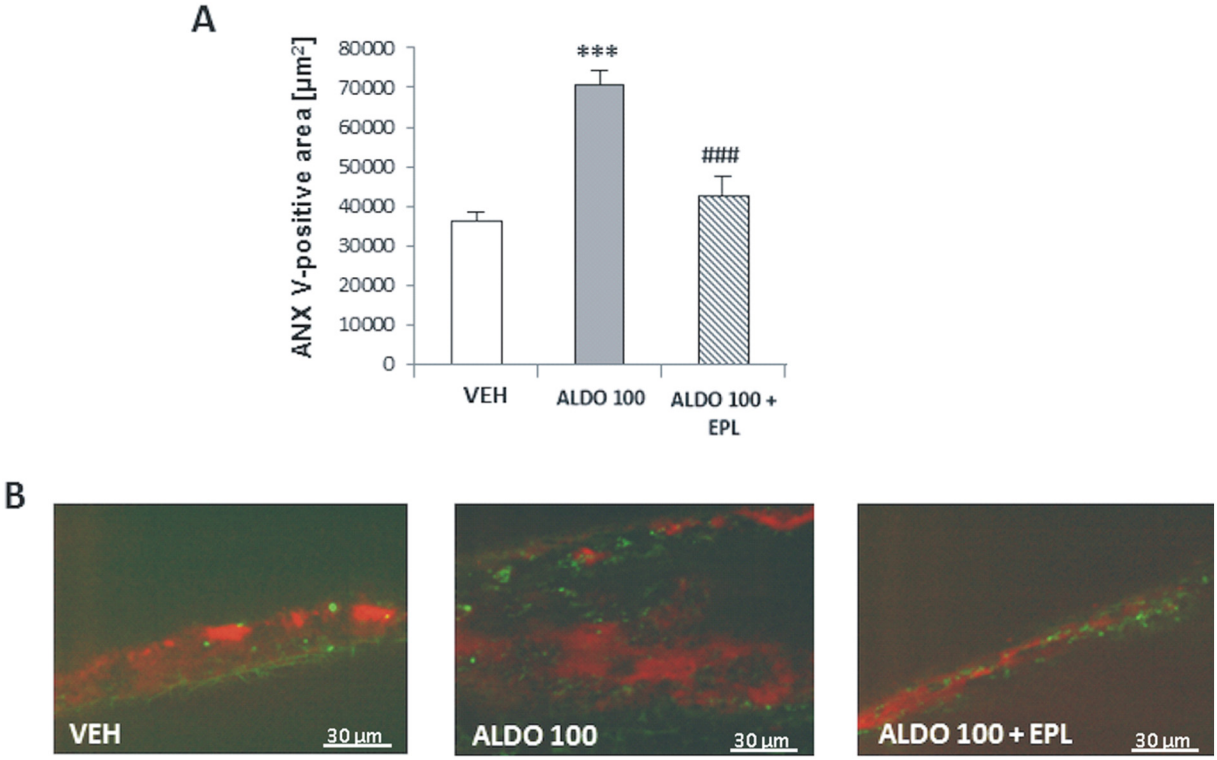

Fig. 4. The effect of aldosterone on irreversible platelet activation in the $FeCl_3$-induced thrombus in wild-type mice: A) expressed as an area of Annexin V (ANX V)-labeled irreversibly activated platelets in the mice treated acutely with vehicle (VEH), aldosterone (ALDO 100 µg/kg), and eplerenone (EPL 100 mg/kg); B) presented as confocal images of the distribution of irreversibly activated platelets (red colour) in the thrombus 2 min after $FeCl_3$-induced injury (representative images, objective 20×). Data are presented as mean ± SEM; ***$p < .001$ *vs* VEH; ###$p < .001$ *vs* ALDO 100; $n = 8$. (For interpretation of the references to colour in this figure legend, the reader is referred to the web version of this article.)

endogenous, mostly platelet-related, thrombin generation. However, the results observed in PPP indicate that platelets are not the only source of acute aldosterone-enhanced thrombin generation. The aldosterone effect may also depend on the microparticles derived from platelets, which are recently proposed to modulate the clot structure to become dense and lysis resistant [36]. Moreover, the lack of aldosterone effect on platelets *in vitro* suggests that aldosterone is not a strong platelet activator *per se*. It seems that the hormone enhances the platelet response to an already initiated process. Previously, it has been shown that aldosterone increased the adhesion of rat platelets to collagen *ex vivo* and has no effect on the aggregation of human platelets *in vitro* [14,37]. Taken together, the different results observed in *ex vivo* and *in vitro* assays suggest that when deprived of the influence of plasma and endothelial factors, the isolated platelets do not respond to aldosterone, but respond strongly when other factors coexist at the bedside.

It seems that the hemostatic factors and signaling elements present in plasma might be more important than platelets in the rapid aldosterone effect on thrombosis augmentation. To confirm the above hypothesis, we performed an *ex vivo* evaluation of coagulation and fibrinolysis with thromboelastometry using whole blood from rats, in the presence of both platelets and plasma. Evaluation of the kinetics of clot formation in the whole blood of rats treated acutely with aldosterone (30 µg/kg) showed no significant effect of the hormone on coagulation. However, a trend toward reduction in CT and CFT was noticed in the aldosterone group. Although, a significant procoagulant effect of the acute infusion of aldosterone (30 µg/kg) was observed in rats in our previous study, since the plasma TF levels in the aldosterone group were fivefold increased [14]. Thromboelastometric measurements showed a strong, MR-dependent delay in fibrinolysis after aldosterone administration. These results are consistent with the finding of the altered clot structure, since the formation of much denser and more cross-linked clots in the presence of aldosterone may result in the formation of thrombi that are more stable mechanically and more resistant to fibrinolysis [38,39].

Disturbed plasma fibrinolysis along with more stable and resistant thrombi may be the result of the endothelial hemostatic imbalance induced by aldosterone. Our experiments with HUVECs stimulated acutely with aldosterone confirmed this hypothesis. Incubation with aldosterone for 10 min was enough to significantly increase the release of procoagulants such as TF, vWF, and antifibrinolytic PAI-1 from endothelial cells, as well as reducing the secretion of profibrinolytic t-PA. Taken together, these extensive effects of the hormone on endothelium-dependent coagulation and fibrinolysis lead to an acute hemostatic imbalance in plasma, fibrinolysis impairment, and finally, prothrombotic state and enhanced thrombosis.

Mouse thrombosis models with intravital imaging finally confirmed that the rapid effects of aldosterone observed *ex vivo* and *in vitro* may occur at the same time *in vivo*, resulting in a rapid interaction of platelets and endothelium that leads to thrombosis enhancement. We chose mouse models, since the intravital imaging for thrombus formation has been used only in the mouse microvasculature so far. It was shown that in laser-induced thrombosis the vascular bed selection has the secondary meaning for the thrombus formation, since laser-injured endothelium is principal to initiate thrombus that is mainly composed of platelets, in both venules and arterioles [30,31,40,41]. Considering the above and the method described by Hayashi et al. [30], as well as the results from our previous study on venous thrombosis [14], we selected mouse mesenteric venules for intravital imaging of thrombus formation. We showed that at a dose of 100 µg/kg aldosterone significantly enhanced platelet accumulation at the site of endothelial injury in mice with laser-induced thrombosis. Interestingly, the highest dose of aldosterone (200 µg/kg) had no prothrombotic effect, although a concomitant increase in blood flow was noticed. We assume that the

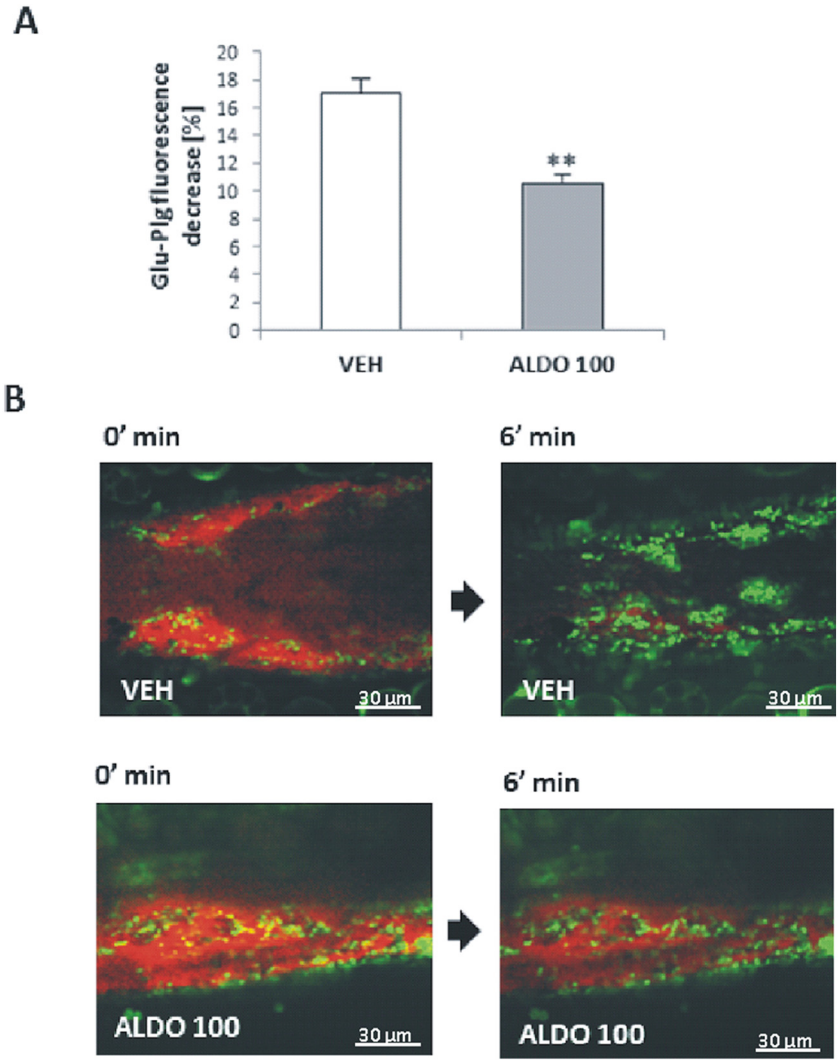

Fig. 5. The effect of aldosterone on Glu-plasminogen (Glu-Plg) fluorescence in the $FeCl_3$-induced thrombus in wild-type mice: A) percent of decrease in Glu-Plg fluorescence within 6 min after thrombosis induction; B) representative confocal images showing the reduction of Glu-Plg fluorescence (red colour) in vehicle (VEH)- and aldosterone (ALDO 100 µg/kg)-treated mice (representative images, objective 20×). Data are presented as mean ± SEM; $^{**}p < .01$ *vs* VEH; $n = 8$. (For interpretation of the references to colour in this figure legend, the reader is referred to the web version of this article.)

hemodynamic changes that occurred after the administration of aldosterone at a dose of 200 µg/kg could be responsible for the weakened thrombus formation, since it was shown that under the highly increased blood flow the thrombus could be eluted [42,43]. The MR blockade with eplerenone did not alter the aldosterone effect, which suggests a more compound mechanism of the aldosterone action in this model, or a stronger injury of the endothelium. Moreover, in the laser-induced thrombosis model, the emission of fluorescence by the formed thrombus was mainly platelet-dependent, although the involvement of neutrophils or monocytes cannot be excluded. Thus, to further investigate the specific role of platelet activation in the mechanism of aldosterone-enhanced thrombosis, the $FeCl_3$-induced thrombosis model was used. This model allowed us to stain the platelets with PS on their surface (PS positive), which is important for the formation of blood coagulation complexes that lead to thrombin generation. According to Hayashi et al., the area of PS-positive platelets corresponds to irreversibly activated platelets with procoagulant activity and correlates with fibrin generation [30]. We confirmed that aldosterone significantly increased the area of irreversibly activated platelets within the developing thrombus, which was reduced by eplerenone. The lack of eplerenone effect on the aldosterone-enhanced platelet accumulation in the laser-induced thrombosis model and the strong antiplatelet effect in the $FeCl_3$-induced thrombosis model could be related to the different functional states of platelets in these two models. The aldosterone-increased platelet activation at the bedside observed in *in vivo* thrombosis models with no effect in *in vitro* tests suggests that the role of platelets in the acute effects of aldosterone on hemostasis is complicated. We assume that platelets could be a target of aldosterone, since the existence of functional MR has been described in human platelets [20]. We also observed the expression of MR at the protein level in rat platelets (data not shown). However, to confirm the role of platelets in the prothrombotic effects of aldosterone, more platelet functional tests should be done.

The results obtained from mice with $FeCl_3$-induced thrombosis that were injected with Glu-plasminogen further suggest that aldosterone weakened fibrinolysis. The conversion of plasminogen to plasmin initiates fibrinolysis. During the progression of fibrinolysis, plasmin (ogen) is expected to diffuse from the fibrin digestion sites within the fibrin degradation products due to continuous blood flow [44]. The poor reduction of Glu-plasminogen fluorescence in the thrombus of aldosterone-injected mice may indicate the attenuated conversion of plasminogen to plasmin. The reason for this weak and ineffective fibrinolysis could be related to the altered clot structure which makes the clot more resistant to fibrinolysis, as well as the reduced amount of t-

PA, the main plasminogen activator. In our previous study, we observed significantly reduced plasma t-PA levels with a simultaneous increase in PAI-1 levels after 1 h of aldosterone infusion in rats [14]. Taking into account the results of our previous and present studies, we assume that the observed aldosterone-enhanced thrombosis with altered clot structure results from the acute procoagulant effect of aldosterone, as well as the reduced plasmin activity due to the reduced level of plasminogen activators and increased level of inhibitors.

5. Conclusion

We have shown that aldosterone acutely enhanced thrombosis. The compound mechanism of the prothrombotic action of aldosterone is related to its rapid, simultaneous effects on platelets, and plasma- and endothelium-dependent hemostatic factors that result in alteration in the structure of clot, making it resistant to fibrinolysis. We assume that the mechanism involves the MR activation and non-genomic signaling, since the aldosterone effects were observed within just 10 min. Understanding the role of the non-genomic pathway and MR in the acute effects of aldosterone in the hemostatic system is essential to explaining the overall mechanism of the hormone action in the cardiovascular system.

Supplementary data to this article can be found online at https://doi.org/10.1016/j.vph.2019.106598.

Funding

This work was supported by the Medical University of Bialystok [grant numbers N/ST/MN/17/002/2226 and N/ST/ZB/18/001/2226].

Author contributions

AG-P designed and performed the experiments, analyzed the data, and drafted the article. NM, AG, and MA performed the experiments and analyzed the data. TM and TR performed the experiments, analyzed the data, and revised the article. EC supervised the research and revised the article.

Disclosure statement

The authors have nothing to disclose.

Declaration of Competing Interest

None declared.

References

[1] C. Grossmann, M. Gekle, New aspects of rapid aldosterone signaling, Mol. Cell. Endocrinol. 308 (2009) 53–62.
[2] P. Coutinho, C. Vega, L.H. Pojoga, A. Rivera, G.N. Prado, T.M. Yao, G. Adler, M. Torres-Grajales, E.R. Maldonado, A. Ramos-Rivera, J.S. Williams, G. Williams, J.R. Romero, Aldosterone's rapid, nongenomic effects are mediated by striatin: a modulator of aldosterone's effect on estrogen action, Endocrinology 155 (2014) 2233–2243.
[3] A.W. Ashton, T.Y. Le, C.E. Gomez-Sanchez, B. McWhinney, A. Hudson, A.S. Mihailidou, Role of nongenomic signaling pathways activated by aldosterone during cardiac reperfusion injury, Mol. Endocrinol. 29 (2015) 1144–1155.
[4] S. Ruhs, A. Nolze, R. Hübschmann, C. Grossmann, 30 years of the mineralocorticoid receptor: nongenomic effects via THE mineralocorticoid receptor, J. Endocrinol. 234 (2017) T107–T124.
[5] O. Skøtt, T.R. Uhrenholt, J. Schjerning, P.B. Hansen, L.E. Rasmussen, B.L. Jensen, Rapid actions of aldosterone in vascular health and disease-friend or foe? Pharmacol. Ther. 111 (2006) 495–507.
[6] A. Mutoh, M. Isshiki, T. Fujita, Aldosterone enhances ligand-stimulated nitric oxide production in endothelial cells, Hypertens. Res. 31 (2008) 1811–1820.
[7] H. Hayashi, M. Kobara, M.K. Abe, N. Tanaka, E. Gouda, H. Toba, H. Yamada, T. Tatsumi, T. Nakata, H. Matsubara, Aldosterone nongenomically produces NADPH oxidase-dependent reactive oxygen species and induces myocyte apoptosis, Hypertens. Res. 31 (2008) 363–375.
[8] P. Gunaruwan, M. Schmitt, J. Sharman, L. Lee, A. Struthers, M. Frenneaux, Effects of aldosterone on forearm vasculature in treated chronic heart failure, Am. J. Cardiol. 95 (2005) 412–414.
[9] P. Scherpereel, D. Robelet, M. Castaner, M.D. Besse, A. Racadot, J. Lefebvre, Postoperative hyperaldosteronism and related endocrine perturbations, Anesth. Analg. 36 (1979) 117–123.
[10] F. Ivanes, S. Susen, F. Mouquet, P. Pigny, F. Cuilleret, K. Sautière, J.P. Collet, F. Beygui, B. Hennache, P.V. Ennezat, F. Juthier, F. Richard, J. Dallongeville, M.A. Hillaert, P.A. Doevendans, B. Jude, M. Bertrand, G. Montalescot, E. Van Belle, Aldosterone, mortality, and acute ischaemic events in coronary artery disease patients outside the setting of acute myocardial infarction or heart failure, Eur. Heart J. 33 (2012) 191–202.
[11] F. Beygui, J.P. Collet, J.J. Benoliel, N. Vignolles, R. Dumaine, O. Barthélémy, G. Montalescot, High plasma aldosterone levels on admission are associated with death in patients presenting with acute ST-elevation myocardial infarction, Circulation 114 (2006) 2604–2610.
[12] A.D. Struthers, Aldosterone: cardiovascular assault, Am. Heart J. 144 (5 Suppl) (2002) S2–S7.
[13] A. Stankiewicz, A. Gromotowicz, J. Szemraj, M. Wojewódzka-Zelezniakowicz, P. Skrzypkowski, E. Chabielska, Acute aldosterone infusion enhances thrombosis development in normotensive rats, Thromb. Haemost. 98 (2007) 697–699.
[14] A. Gromotowicz, J. Szemraj, A. Stankiewicz, A. Zakrzeska, M. Mantur, E. Jaroszewicz, F. Rogowski, E. Chabielska, Study of the mechanisms of aldosterone prothrombotic effect in rats, J. Renin-Angiotensin-Aldosterone Syst. 12 (2011) 430–439.
[15] A. Gromotowicz-Poplawska, A. Stankiewicz, K. Kramkowski, A. Gradzka, M. Wojewodzka-Zelezniakowicz, J. Dzieciol, J. Szemraj, E. Chabielska, The acute prothrombotic effect of aldosterone in rats is partially mediated via angiotensin II receptor type 1, Thromb. Res. 138 (2016) 114–120.
[16] P. Pearce, J.W. Funder, High affinity aldosterone binding sites (type I receptors) in rat heart, Clin. Exp. Pharmacol. Physiol. 14 (1987) 859–866.
[17] M. Lombès, N. Alfaidy, E. Eugene, A. Lessana, N. Farman, J.P. Bonvalet, Prerequisite for cardiac aldosterone action. Mineralocorticoid receptor and 11 beta-hydroxysteroid dehydrogenase in the human heart, Circulation 92 (1995) 175–182.
[18] W.J. Meyer 3rd, N.R. Nichols, Mineralocorticoid binding in cultured smooth muscle cells and fibroblasts from rat aorta, J. Steroid Biochem. 14 (1981) 1157–1168.
[19] J.W. Funder, P.T. Pearce, R. Smith, J. Campbell, Vascular type I aldosterone binding sites are physiological mineralocorticoid receptors, Endocrinology 125 (1989) 2224–2226.
[20] L.A. Moraes, M.J. Paul-Clark, A. Rickman, R.J. Flower, N.J. Goulding, M. Perretti, Ligand-specific glucocorticoid receptor activation in human platelets, Blood 106 (2005) 4167–4175.
[21] D. Sztechman, K. Czarzasta, A. Cudnoch-Jedrzejewska, E. Szczepanska-Sadowska, T. Zera, Aldosterone and mineralocorticoid receptors in regulation of the cardiovascular system and pathological remodelling of the heart and arteries, J. Physiol. Pharmacol. 69 (6) (2018), https://doi.org/10.26402/jpp.2018.6.01.
[22] M. Caprio, B.G. Newfell, A. la Sala, W. Baur, A. Fabbri, G. Rosano, M.E. Mendelsohn, I.Z. Jaffe, Functional mineralocorticoid receptors in human vascular endothelial cells regulate intercellular adhesion molecule-1 expression and promote leukocyte adhesion, Circ. Res. 102 (2008) 1359–1367.
[23] T. Misztal, T. Rusak, J. Branska-Januszewska, H. Ostrowska, M. Tomasiak, Peroxynitrite may affect fibrinolysis via the reduction of platelet-related fibrinolysis resistance and alteration of clot structure, Free Radic. Biol. Med. 89 (2015) 533–547.
[24] R.J. Luddington, Thrombelastography/thromboelastometry, Clin. Lab. Haematol. 27 (2005) 81–90.
[25] M.J. Mant, Platelet adherence to collagen: a simple, reproducible, quantitative method for its measurement, Thromb. Res. 11 (1977) 729–737.
[26] J.D. Sweeney, J.W. Labuzzetta, C.E. Michielson, J.E. Fitzpatrick, Whole blood aggregation using impedance and particle counter methods, Am. J. Clin. Pathol. 92 (1989) 794–797.
[27] N. Marcinczyk, D. Jarmoc, A. Leszczynska, A. Zakrzeska, K. Kramkowski, J. Strawa, A. Gromotowicz-Poplawska, E. Chabielska, M. Tomczyk, Antithrombotic potential of tormentil extract in animal models, Front. Pharmacol. 8 (2017) 534.
[28] K. Przyborowski, H. Kassassir, M. Wojewoda, K. Kmiecik, B. Sitek, K. Siewiera, A. Zakrzewska, A.M. Rudolf, R. Kostogrys, C. Watala, J.A. Zoladz, S. Chlopicki, Effects of a single bout of strenuous exercise on platelet activation in female ApoE/LDLR(−/−) mice, Platelets. 28 (2017) 657–667.
[29] R.I. Freshney, Culture of Animal Cells: A Manual of Basic Technique and Specialized Applications, Alan R. Liss, Inc., 1987.
[30] T. Hayashi, H. Mogami, Y. Murakami, T. Nakamura, N. Kanayama, H. Konno, T. Urano, Real-time analysis of platelet aggregation and procoagulant activity during thrombus formation in vivo, Pflugers Arch. 456 (2008) 1239–1251.
[31] S. Falati, P. Gross, G. Merrill-Skoloff, B.C. Furie, B. Furie, Real-time in vivo imaging of platelets, tissue factor and fibrin during arterial thrombus formation in the mouse, Nat. Med. 8 (2002) 1175–1181.
[32] J. Galvao, B. Davis, M. Tilley, E. Normando, M.R. Duchen, M.F. Cordeiro, Unexpected low-dose toxicity of the universal solvent DMSO, FASEB J. 28 (2014) 1317–1330.
[33] P. Montaguti, E. Melloni, E. Cavalletti, Acute intravenous toxicity of dimethyl sulfoxide, polyethylene glycol 400, dimethylformamide, absolute ethanol, and benzyl alcohol in inbred mouse strains, Arzneimittelforschung 44 (1994) 566–570.
[34] A. Eckly, B. Hechler, M. Freund, M. Zerr, J.P. Cazenave, F. Lanza, P.H. Mangin, C. Gachet, Mechanisms underlying $FeCl_3$-induced arterial thrombosis, J. Thromb. Haemost. 9 (2011) 779–789.
[35] C. Whyte, F. Swieringa, T.G. Mastenbroek, A.S. Lionikiene, M.D. Lancé, P.E. van der Meijden, J.W. Heemskerk, N.J. Mutch, Plasminogen associates with

phosphatidylserine-exposing platelets and contributes to thrombus lysis under flow, Blood 125 (2015) 2568–2578.
[36] L.D. Zubairova, R.M. Nabiullina, C. Nagaswami, Y.F. Zuev, I.G. Mustafin, R.I. Litvinov, J.W. Weisel, Circulating microparticles alter formation, structure, and properties of fibrin clots, Sci. Rep. 5 (2015) 17611.
[37] A. Schäfer, D. Fraccarollo, S. Hildemann, M. Christ, M. Eigenthaler, A. Kobsar, U. Walter, J. Bauersachs, Inhibition of platelet activation in congestive heart failure by aldosterone receptor antagonism and ACE inhibition, Thromb. Haemost. 89 (2003) 1024–1030.
[38] T. Rusak, J. Piszcz, T. Misztal, J. Brańska-Januszewska, M. Tomasiak, Platelet-related fibrinolysis resistance in patients suffering from PV. Impact of clot retraction and isovolemic erythrocytapheresis, Thromb. Res. 134 (2014) 192–198.
[39] L.W. Chan, N.J. White, S.H. Pun, A fibrin cross-linking polymer enhances clot formation similar to factor concentrates and tranexamic acid in an in vitro model of coagulopathy, ACS Biomater. Sci. Eng. 2 (2016) 403–408.
[40] L. Bellido-Martín, V. Chen, R. Jasuja, B. Furie, B.C. Furie, Imaging fibrin formation and platelet and endothelial cell activation in vivo, Thromb. Haemost. 105 (2011) 776–782.
[41] M.J. Kuijpers, J.W. Heemskerk, Intravital imaging of thrombus formation in small and large mouse arteries: experimentally induced vascular damage and plaque rupture in vivo, Methods Mol. Biol. 788 (2012) 3–19.
[42] B.M. Schmidt, S. Oehmer, C. Delles, R. Bratke, M.P. Schneider, A. Klingbeil, E.H. Fleischmann, R.E. Schmieder, Rapid nongenomic effects of aldosterone on human forearm vasculature, Hypertension 42 (2003) 156–160.
[43] L.F. Brass, S.L. Diamond, Transport physics and biorheology in the setting of hemostasis and thrombosis, J. Thromb. Haemost. 14 (2016) 906–917.
[44] C. Longstaff, K. Kolev, Basic mechanisms and regulation of fibrinolysis, J. Thromb. Haemost. 13 (Suppl. 1) (2015) S98–S105.